

Development and Analysis of an In-Mold Coating Procedure for Thermoplastic Resin Transfer Molding to Produce PA6 Composites with a Multifunctional Surface

Orsolya Viktória Semperger^{1,2}, Dániel Török¹, András Suplicz^{1,3*}

¹ Department of Polymer Engineering, Faculty of Mechanical Engineering, Budapest University of Technology and Economics, Műegyetem rkp. 3, H-1111 Budapest, Hungary

² Production Division, Bay Zoltán Nonprofit Ltd. for Applied Research, Kondorfa utca 1., H-1116 Budapest, Hungary

³ MTA-BME Lendület Lightweight Polymer Composites Research Group, Műegyetem rkp. 3., H-1111 Budapest, Hungary

* Corresponding author, e-mail: suplicz@pt.bme.hu

Received: 22 August 2022, Accepted: 10 September 2022, Published online: 19 September 2022

Abstract

We have developed a complex Thermoplastic Resin Transfer Molding procedure to create polyamide 6 composites and their multifunctional coatings in a single production cycle with low cycle time. The advantage of the new process is that it has low emission of volatile organic compounds due to the closed mold and the products can be recycled easily, decreasing the negative impact on the environment. In addition to developing the process steps and parameters, we produced samples with different curing time and fabric content of the base layer, waiting time before coating injection, surface thickness and titanium dioxide content of the surface layer. Then we analyzed the adhesion between the surface and base layers and the warpage of the complex part. SEM analysis proved that the reinforcement fabrics could be properly impregnated with the reactive thermoplastic system during the production of the base layer. Furthermore, we showed that the strength of the interlayer bonding can be improved when the base layer is properly polymerized in the first step. Using our method developed to assess warpage, we demonstrated that the warpage of the base layer can be reduced by applying the appropriate manufacturing parameters to the surface layer.

Keywords

Thermoplastic RTM, In-Mold Coating, anionic ring-opening polymerization, adhesion, warpage

1 Introduction

With the continuous development of the plastics industry, the diversity of raw materials and applicable manufacturing technologies has increased significantly. At the same time, unfortunately, the amount of plastic waste generated at the end of the lifetime of the product is also increasing. Therefore, more and more directives (e.g., in the European Union) are now regulating the recycling of plastic products in accordance with the circular economy. In addition to recyclability, sustainability in plastics strategies also includes designing and using polymer products [1, 2]. As a result, thermoplastics are becoming more and more important in composite technology [3–6]. Short-fiber composite products have long been produced by injection molding and extrusion, but the combination of continuous reinforcement structures and thermoplastic matrix materials has only recently become more common. Typical examples are organosheets, tapes, or products produced

by the increasingly researched T-RTM (Thermoplastic Resin Transfer Molding) technology [7–11].

Thermoplastic RTM is a process for the economical production of composite products with a continuous reinforcement structure and complex geometry. The process involves infusing the reinforcing fabric in the mold with a low-viscosity reactive thermoplastic system, which is polymerized at high temperatures in a closed mold. Much research has been directed toward the development of polyamide 6 (PA6) matrix composites that can be produced in this way. In this case, the starting monomer is ϵ -caprolactam, which has a viscosity of well below 1 Pas in the molten state [12, 13]. It is most commonly processed in combination with a C10/C20P initiator/activator combination (sodium caprolactam and hexamethylene-1,6-carbamoyl caprolactam, respectively), which makes it possible to complete the anionic ring-opening polymerization

in a few minutes (~5 minutes) [14]. The process is typically performed below the melting point of PA6 (130–180 °C), resulting in a high degree of conversion (nearly 100%) and crystalline fraction (~40–45%) [15, 16]. Previous research mainly focused on the type and ratio of initiator/activator [17–19], the impregnation of the reinforcing structure [20, 21], and the analysis of the properties of the composites produced [21–23]. As with the conventional RTM (Resin Transfer Molding) process, a major drawback of this technology is that the properties of the matrix material (flame retardancy, UV stability, toughness, etc.) cannot be modified by the addition of fillers. The reinforcement filters out the filler particles, causing local inhomogeneities. Surface coating can be a solution to this problem [24].

The composite parts undergo some post-treatment before use, which modify their surface properties. It is possible to modify their appearance (coloring) or even their UV, water, corrosion, etc. resistance. Coatings can be produced on polymer products with several methods [25, 26]. Painting is the easiest (dipping, spraying, brushing, film casting, etc.), but this is only possible after proper surface preparation (degreasing, roughening, adhesion improvement) due to the relatively low surface energy of polymeric materials. In most cases, these processes involve different materials for the base, coupling, and coating layers, which complicates the recyclability of complex products and typically results in high VOC (Volatile Organic Compounds) emissions [27]. A solution to this problem is In-Mold Coating (IMC), which is mainly used in compression molding, injection molding or conventional RTM [28, 29]. During the process, the coating is created in a closed mold, thus environmental regulations are met and the difficulties and additional costs associated with surface treatment are reduced. The coating and the product are produced directly one after the other, and no post-processing is required [30, 31]. IMC can be performed by placing the coating layer in the mold or by partially opening the mold and injecting the surface material [29–33].

Also, in the case of Thermoplastic RTM, there is a great demand for a surface coating process that achieves low VOC emissions and does not significantly increase production cycle time. To this end, we have developed an In-Mold Coating process for T-RTM, to create a multifunctional surface with the same base material (polyamide 6) by in-situ polymerization within one production cycle. In this way, the composites can meet both environmental (recyclability) and automotive (high strength, modified surface, flame retardancy, UV and scratch resistance etc.) requirements of

the 21st century. Using the process developed, we prepared samples with different parameters. Then we analyzed the effect of reaction times, layer thicknesses, reinforcement content and filler content on adhesion between the layers, and the warping of the whole product.

2 Materials and methods

2.1 Materials

The polyamide 6 test specimens were prepared from an ϵ -caprolactam–initiator–activator system by anionic ring opening polymerization. The in-situ polymerization took place below the melting point (130–175 °C) of PA6. AP-Nylon ϵ -caprolactam (CL, L. Brüggemann GmbH & Co. KG, Germany) was used as the monomer, whose melting point is 69 °C, its density in the melt state is 1.01 g/cm³, and its viscosity is 3–5 mPas. Sodium caprolactamate (Brüggolen C10, L. Brüggemann GmbH & Co. KG, Germany) was used as initiator. Its melting point is 62.2 °C and its density in the melt state is 1.02 g/cm³. Hexamethylene-1,6-dicarbonyl caprolactam (Brüggolen C20P, L. Brüggemann GmbH & Co. KG, Germany) was used as activator. Its melting point is 70 °C and its density in the melt state is 1.02 g/cm³. The CL was 92.5 wt%, C10 was 4.5 wt% and C20P was 3 wt%. They were stored under vacuum due to their high moisture absorption capacity. The maximum moisture content of the raw materials can be <0.01%.

Glass fiber (StarRov 895, Johns Manville GmbH, Germany) was used as reinforcement, which had surface treatment compatible with polyamide 6. It is plain-woven and its density is 800 g/m². Furthermore, 99.5% pure, rutile titanium dioxide (nTiO₂, SkySpring Nanomaterials Inc., USA) was used as filler in the surface layer. Its particle size is 10–30 nm and it has APS surface treatment. We dried the fabric and the filler at 80 °C for 8 hours to remove moisture.

2.2 Processing method

We used a T-RTM machine manufactured by KraussMaffei (Munich, Germany) and a mold that our research group had designed [34] to prepare the test specimens. The equipment consists of two dosing units (DU) and a hydraulic press. The first dosing unit (DU1) is used for the base and the second unit (DU2) for surface coating. The hydraulic press is used to move the upper mold half (opening and closing) and to provide the clamping force during the process. The right amount of ingredients were measured and added to the DU as a preparatory step. The appropriate amount of fillers was loaded into the second dosing unit to

the C20P and the ε -caprolactam. The activator (CL+C20P) and initiator (CL+C10) components, loaded in separate melting tanks, were melted at 110 °C under a vacuum. During operation, the melt was continuously circulated in a closed loop to avoid contact with outside air, due to the hydrophilic nature of the raw materials.

2.3 Design of experiments

The constant manufacturing parameters used in production are listed in Table 1.

We prepared test specimens with different process parameters and conditions based on a design of experiment to investigate their effect on the IMC (In-Mold Coating) process and the adhesion between the layers. The variable parameters used in the sample preparation were:

- curing time of the base layer (waiting time): 70; 120; 180 s,
- waiting time before the injection of the coating: 0 or 5 min,
- surface thickness: 0.15 mm (30 g); 0.3 mm (60 g); 0.6 mm (100 g)
- nTiO₂ content of the surface layer: 0 wt%; 0.5 wt%; 1 wt%
- fabric content of the base: without fabric; with fabric.

2.4 Characterization of the samples

2.4.1 ATR–FTIR analysis

The chemical composition of the samples was analyzed by Attenuated Total Reflectance Fourier Transform Infrared Spectroscopy (ATR-FTIR), with a Bruker Tensor II apparatus (Bruker Optics Inc., Billerica, MA). It was equipped with a Specac Golden Gate ATR unit (Specac Ltd., Orpington, UK). We analyzed the absorbances in the wavelength range from 4000 to 400 cm⁻¹. Sixteen scans were performed and averaged on each sample.

Table 1 Main production parameters

Parameters	Value	Unit
Mold temperature	150	°C
Mold closing pressure	30	bar
Polymerization (curing) time of the base layer (with surface/without surface)	120/180	s
Polymerization (curing) time of the surface layer	180	s
Melt temperature	110	°C
Injection rate	35	g/s
Vacuuming time (mold)	30	s

2.4.2 Scanning Electron Microscopy

The structure of the prepared composites and the infiltration of the fabric was investigated with SEM (Scanning Electron Microscopy) micrographs with the use of a JEOL JSM 6380LA electron microscope. Before the measurement, the specimens were coated with an Au/Pd alloy, which eliminates undesirable electrostatic charging.

2.4.3 Adhesion test

The adhesion of coatings was tested with a PosiTest ATM20A (DeFelsko, Ogdensburg, USA) pull-off adhesion tester, according to the EN ISO 4624 standard (Fig. 1). We used aluminum dollies with a diameter of 20 mm for the measurements. The first step was to clean the surface of the specimen with Loctite SF 7063 cleaner, and the dollies were glued to the surface with Loctite Super Bond Power Flex Gel adhesive. After 24 hours, a cutting tool was used to cut the coating layer around the test area and the clamps were pulled off the surface with a hydraulic puller. From the measured forces, the equipment automatically calculated the pull-off strength.

2.4.4 Part deflection analysis method

The different degrees of shrinkage of the base and the coating, and the successive formation of the two layers, can lead to the product's warpage. To analyze the level of this deformation, we developed a measurement method based on 3D scanning and data analysis. It allows us to measure the degree of deviation from the ideal geometry. First, we scanned the surface of the specimens using a GOM ATOS Core 5M 3D scanner. After that, the scanned point clouds were loaded into MATLAB software for further manipulation. Firstly we performed the orientation of the specimens to make them comparable. To do this, we fitted a reference plane with the least squares method to the points of the 0–10 mm band next to the flow aid (Fig. 2).

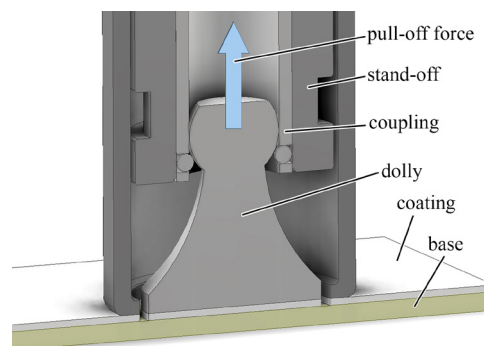


Fig. 1 Layout of the adhesion test (cross-section)

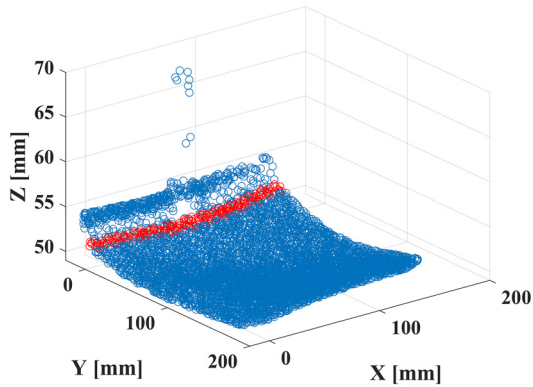


Fig. 2 Creating the reference plane

The reference plane was given with (Eq. (1)):

$$Z = p_1 + p_2 \times X + p_3 \times Y \quad (1)$$

where p_1 , p_2 and p_3 were the fitting parameters.

Next, an offset was performed in the Z direction, then rotation around the X , Y , Z axis. For the offset, the X , Y and Z coordinates of the scanned point were multiplied with the following transformation matrix (Eq. (2)):

$$T = \begin{bmatrix} 1 & 0 & 0 & 0 \\ 0 & 1 & 0 & 0 \\ 0 & 0 & 1 & 0 \\ \Delta X & \Delta Y & \Delta Z & 1 \end{bmatrix} \quad (2)$$

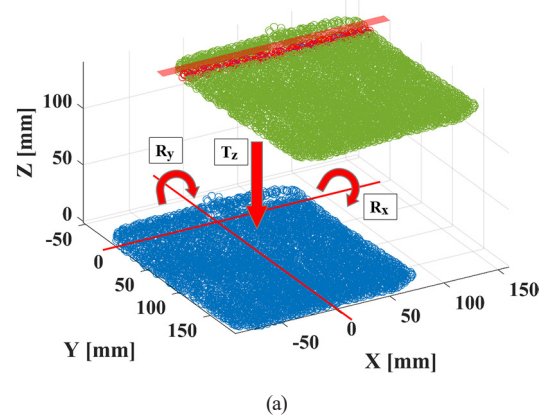
where $\Delta X = 0$, $\Delta Y = 0$, $\Delta Z = p_1$. Next, the point cloud was rotated around the X , Y , Z axis with use of the following rotation matrices (Eq. (3)–(5)):

$$R_x = \begin{bmatrix} 1 & 0 & 0 & 0 \\ 0 & \cos(\alpha) & \sin(\alpha) & 0 \\ 0 & -\sin(\alpha) & \cos(\alpha) & 0 \\ 0 & 0 & 0 & 1 \end{bmatrix} \quad (3)$$

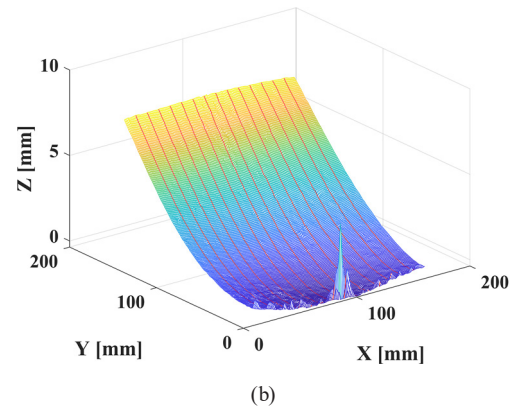
$$R_y = \begin{bmatrix} \cos(\beta) & 0 & \sin(\beta) & 0 \\ 0 & 1 & 0 & 0 \\ -\sin(\beta) & 0 & \cos(\beta) & 0 \\ 0 & 0 & 0 & 1 \end{bmatrix} \quad (4)$$

$$R_z = \begin{bmatrix} \cos(\gamma) & \sin(\gamma) & 0 & 0 \\ -\sin(\gamma) & \cos(\gamma) & 0 & 0 \\ 0 & 0 & 1 & 0 \\ 0 & 0 & 0 & 1 \end{bmatrix} \quad (5)$$

where $\alpha = \arctan(p_3)$, $\beta = \arctan(p_2)$, $\gamma = 0$. As the specimens were always placed in the same position on the table of the 3D scanner, rotation was only required around the X and Y axes, and offset only in the Z direction (Fig. 3 (a)).



(a)



(b)

Fig. 3 Orientation of the point cloud (a) and the regular mesh generated from the points (b)

After setting the appropriate orientation, we generated a regular mesh from the point cloud with a resolution of 1 mm and equal spacing in the X and Y directions. The mesh was partitioned along the Y -axis with parallel planes at 10 mm intervals (Fig. 3 (b)). The deformation of the samples was evaluated with the help of these partitions.

3 Results and discussion

3.1 Development of an In-Mold Coating process for Thermoplastic RTM

To create fiber-reinforced thermoplastic composites with a surface layer within one production cycle, we have developed an IMC (In-Mold Coating) process for T-RTM. The main steps of this procedure are shown in Fig. 4. The first step is inserting the pre-formed reinforcing structures into the mold (step 1). In the second step, the mold is closed until the production position is reached, then the sealed mold cavity is vacuumed (~ 500 mbar) (step 2). Vacuuming the mold is essential to remove air and moisture from the cavity so that perfect filling can be achieved. In the third step, the first dosing unit (DU1) starts the injection cycle of the base layer, during which the mixing head mixes the activator and initiator components of the ϵ -caprolactam monomer, followed by the impregnation

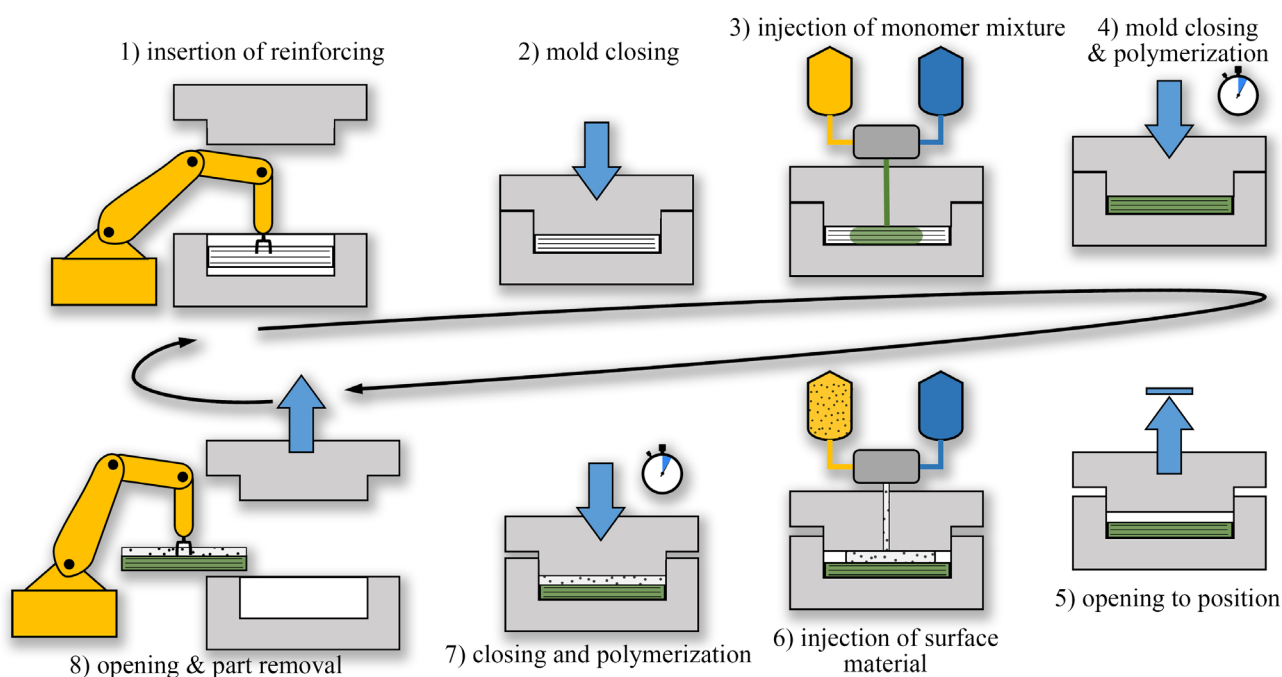


Fig. 4 The In-Mold Coating process that we developed for T-RTM

of the reinforcement structure (step 3). In the fourth step, the press produces the set die pressure, and the anionic polymerization of the base layer begins (step 4). After the curing time has elapsed, the mold is partially opened to the preset position so that the surface layer can be injected (step 5). Subsequently, the second dosing unit (DU2) starts the surface layer injection cycle and injects the ϵ -caprolactam–initiator/ ϵ -caprolactam–activator–filler mixtures into the mold through the mixing head (step 6). When the injection is completed, the curing time starts so that a conversion close to 100% can be reached (step 7). During the polymerization process, the mold maintains a preset force so that it is in continuous contact with the product, despite shrinkage, to ensure contact heating and a uniform surface. Finally, the mold is opened, and the finished product is removed from the mold (step 8).

3.2 Evaluation of the applicability of the technology

One of the critical steps in the IMC process is to create the space for the coating (Fig. 4, step 5). The coating separated from the base layer when the mold was fully opened and then closed back into position (Fig. 5 (a)). The same happened when a previously produced base was placed in the mold for coating. Although the polymerization of both the base and the coating layer was adequate, there were ϵ -caprolactam crystals at the interface. When the mold was only partially opened (according to Fig. 4), the sealed

mold prevented the base layer from coming into contact with the ambient air. In this case, adhesion between the layers was adequate (Fig. 5 (b)).

We performed ATR-FTIR (Attenuated Total Reflectance Fourier Transform Infrared Spectroscopy) studies on the samples with poor adhesion (Fig. 6), and showed that both the surface and the base layer had characteristic peaks typical of polyamide 6: hydrogen-bonded N–H stretching at 3295 cm^{-1} , C–H stretching and tension vibration at 2924 and 2854 cm^{-1} , respectively, amide I (C=O) vibration at 1634 cm^{-1} and amide II (N–H and C–N combination) vibration at 1537 cm^{-1} [35, 36]. For the samples taken from



Fig. 5 Samples with low (a) and good surface adhesion (b)

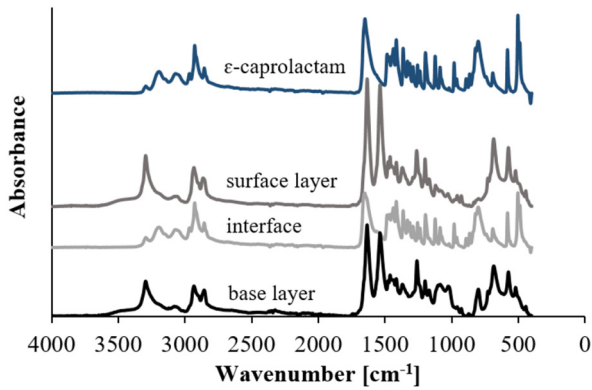


Fig. 6 ATR-FTIR spectra of the coated sample with low surface adhesion

the interface, we clearly showed that poor polymerization took place there. We obtained bonds typical of ϵ -caprolactam, which the methyl alkyl group groups characterize well ($-\text{CH}_2-$, from cyclic lactam), appearing between 3500 and 2750 cm^{-1} [37].

The poor conversion at the interface and thus the adhesion failure can be explained with the hydrophilic nature of polyamide 6, which blocks the polymerization process in regions close to the surface [19, 38]. Our previous measurements show that PA6 prepared by anionic ring-opening polymerization can absorb approximately 0.05% moisture at 50% relative humidity in one hour [39]. This value refers to the whole sample due to the nature of the measurement. Thus, due to diffusion processes, the actual concentration near the surface is much higher than this, inhibiting polymerization [19] and proper adhesion.

Another critical step in T-RTM is to properly impregnate the reinforcing structure. Otherwise, mechanical properties are impaired. In our process, proper impregnation is facilitated by the low viscosity of the monomer blends, the vacuum in the cavity, and the high cavity pressure (30 bar) applied. We took SEM micrographs of the cross-section of the composite sample (Fig. 7) to verify their quality and proved that the matrix material properly infiltrated the rovings. Also, the image shows that the matrix wetted the fiber surface sufficiently, and good adhesion was achieved.

The quality of the boundary layer between the base and the coating was also analyzed by SEM (Fig. 8). Although the base and surface layers can be separated well due to the reinforcement structure used, no clear interface or boundary layer can be found. During the polymerization of the coating, the growing molecular chains were able to attach to the chains on the surface of the base layer, thus creating a strong bond.

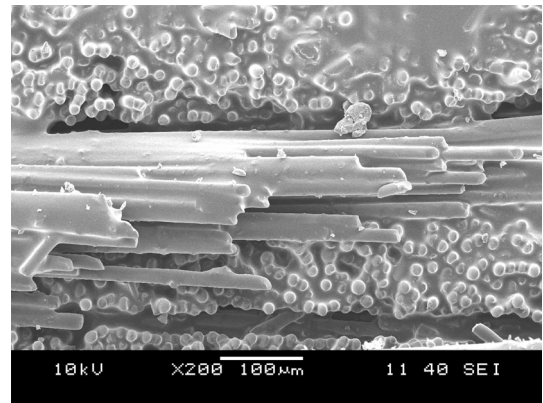


Fig. 7 SEM micrograph of the cross-section of the composite sample (infiltration of the reinforcements in the base layer)

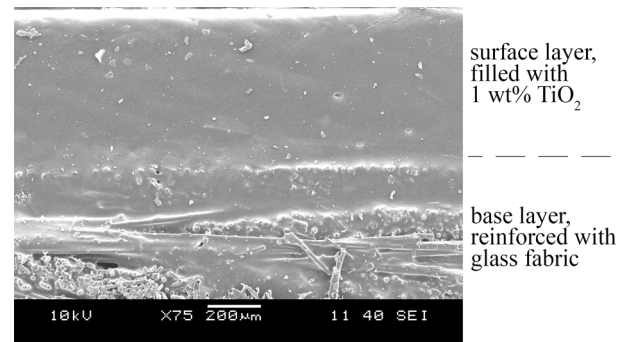


Fig. 8 SEM micrograph of the cross-section of the coated sample

3.3 Adhesion of the coating layer

The adhesion strength between the base layer and the surface coating produced by the IMC method we developed is shown in Fig. 9 as a function of surface layer thickness and the reaction time of the base layer. The reaction times of the base layer were determined according to the following criteria: at 70 s, the pressure sensor in the mold reaches 0 bar, which means that the specimen starts to solidify and shrink away from the mold wall. Furthermore, in our preliminary experiments, we also produced test pieces in 120 and 180 s with similar conversion rates and crystalline fractions at the same mold temperatures [15]. We specified

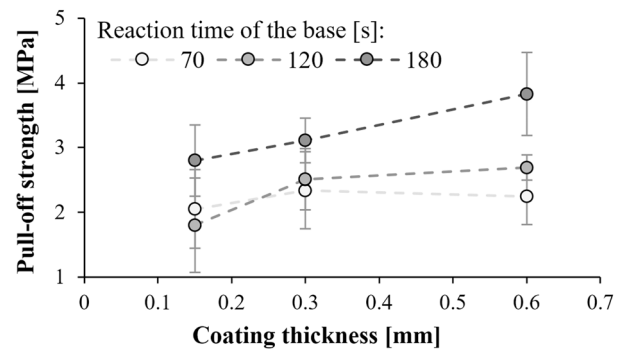


Fig. 9 Pull-off strength as a function of surface layer thickness and the reaction time of the base layer

a shorter polymerization (curing) time of the preform (70 and 120 s) to achieve better adhesion and speed up the production cycle. Despite the uncertainty of measurement, Fig. 9 shows that adhesion strength increases with increasing reaction time of the base layer. This is explained by the fact that 70 s is not sufficient for the complete polymerization reaction, and therefore the newly arriving 110 °C coating reactive thermoplastic system can freeze the reactions on the surface, thus shortening the molecular chains [40]. However, polymerization completes in 180 s, so it can no longer be influenced by the temperature of the injected surface material. Furthermore, adhesion strength also improves with increasing thickness of the surface layer. One reason for this can be that as coating thickness increases, the overall thickness of the sample increases, therefore it is less deformed during pull-off. Smaller deformation results in a more uniform stress distribution on the bonded surface.

Fig. 10 shows the pull-off strength as a function of surface layer thickness and the waiting time before coating. The graph also supports our finding that interlayer adhesion improves with increasing base layer conversion. For a surface layer thickness of 0.6 mm, the pull-off strength increased by nearly 60% with the addition of a five-minute waiting time.

We also investigated the adhesion between the surface layer with 0.5 and 1 wt% nano-sized TiO₂ particles, and the base layer (Fig. 11). TiO₂ is a widely used filler for polymers. It is an inexpensive and non-toxic semiconductor, and it enhances the properties of polymers. It can enhance UV stabilization, strength and antibacterial activity [41]. In the present work, our goal was to investigate how this filler affects the bonding between the two layers. For the surface layers without filler, tear strength increases with increasing layer thickness. At the same time, the values obtained for the surfaces with filler did not change significantly.

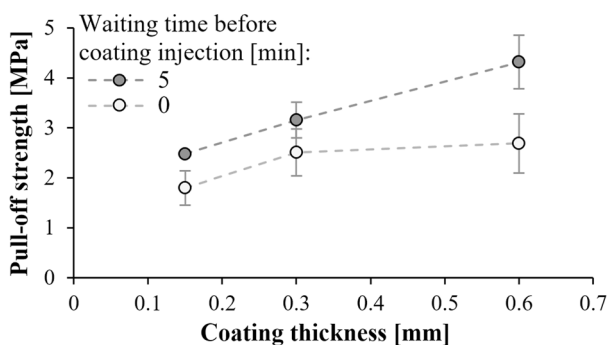


Fig. 10 Pull-off strength as a function of the surface layer thickness and the waiting time before coating injection

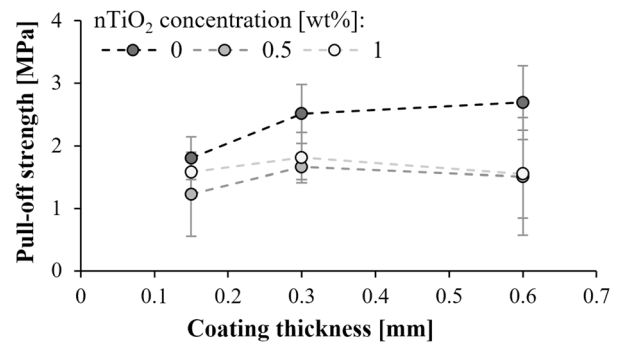


Fig. 11 The effect of a surface layer containing TiO₂ on the quality of adhesion

Furthermore, the addition of a filler can weaken the adhesion between the base and surface layers. The filler can reduce the effective area of adhesion on the contact surface and gaps can be created along the particles.

We also investigated the effect of the continuous glass fiber reinforcement on the interlaminar adhesion of the coated samples. The fiber content was 68.2% ±0.17%. In this case, we prepared a 0.15 mm thick coating layer on the surface of the reinforced base layer. The coating contained 0 and 1 wt% nano-sized TiO₂ particles. Fig. 12 shows the measurement results. A 25% higher tear strength was obtained for the samples containing glass fabric. It is also due to the higher stiffness and lower deformation of the composite base and surface layer.

3.4 Deformation of the samples

Although the base and the surface layer are manufactured within the same cycle, their production can be well separated in time. Thus, the shrinkage of the different layers during polymerization and crystallization can cause warpage. To analyze the warpage of the complex part, we investigated the displacement of the centerline of the part in the Z direction using the method described. The explanation of deformation directions is presented in Fig. 13.

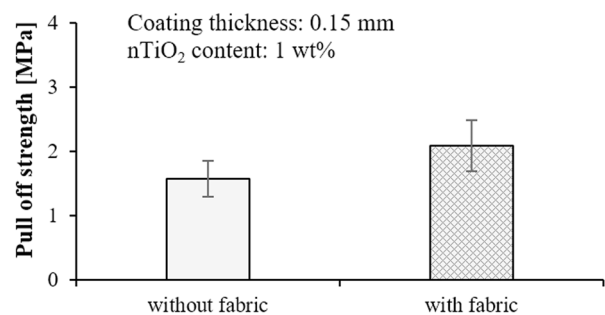


Fig. 12 Effect of the glass fabric reinforcement on the pull-off strength of the coating

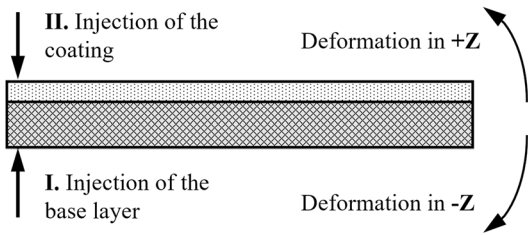


Fig. 13 Explanation of deformation directions

First, we investigated the effect of the thickness of the coating (Fig. 14). Unfortunately, the samples prepared without coating were also significantly warped. This may be due to the different rates of polymerization of the two sides, which are affected by the tempering channels of the mold. Furthermore, smaller coating thicknesses do not significantly affect the longitudinal deformation of the specimens. One reason for this is that the stress resulting from the shrinkage of the coating could not deform the thicker and stiffer base layer, which already had a high conversion rate. Another reason for this phenomenon is that the subsequently injected thin surface layer heated up rapidly to the polymerization temperature (150 °C) and polymerized and crystallized rapidly, thus shrinking together with the base layer.

In the case of the 0.6 mm thick coating, the deformation of the sample in the Z direction is much smaller than that of the reference sample. This thick layer heated up more slowly to the polymerization temperature so that polymerization and crystallization started later, thus the thick layer shrinks later than the base layer. So a surface layer of 0.6 mm is already sufficient to produce a nearly flat product.

Furthermore, we examined the effect of the glass fabric content of the base layer on the warpage of the samples (Fig. 15). In these experiments, the surface layer contained 1 wt% nTiO₂. As Fig. 15 shows, the warpage of the samples containing reinforcements is negligible, while the warpage of the pure polyamide 6 samples is more significant.

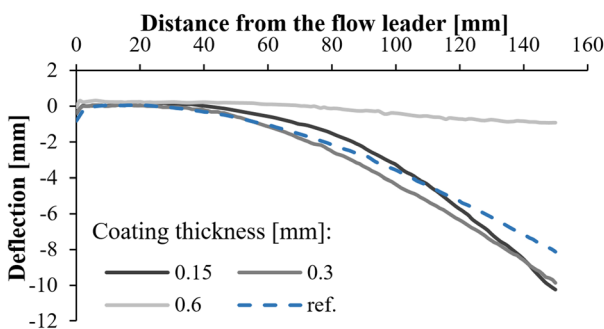


Fig. 14 Warpage of the specimens as a function of coating thickness

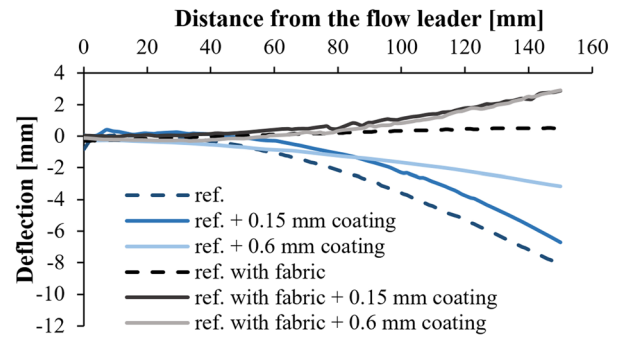


Fig. 15 Effect of the reinforcement and coating thickness on the deflection of the specimen

In the case of the unreinforced base layers, the surface layers reduced the warpage in all cases. In the case of a 0.6 mm coating, the warpage of the polyamide 6 sample is compensated for by the surface layer and approaches a completely flat surface. The reinforced samples were warped in the positive Z direction, so the surface increased deflection. In this case, the effect of the thickness of the surface layer was negligible. A maximum deflection of about 2.8 mm was measured for both 0.15 and 0.6 mm thick surfaces.

Fig. 16 shows the deflection of the centerline of the samples with a 0.15 mm thick surface layer with different TiO₂ contents. This low filler content does not significantly affect the warping of the samples. This is likely to be a combination of two factors. The first is that TiO₂ can slightly increase the crystalline proportion of the samples, which increases shrinkage due to the more ordered structure. The opposite effect is that the presence of filler improves dimensional stability. Total warpage can result from the sum of the two effects and depends on their proportion. As filler content increases, warping also decreases, which can be attributed to an increase in the stiffness of the surface layer.

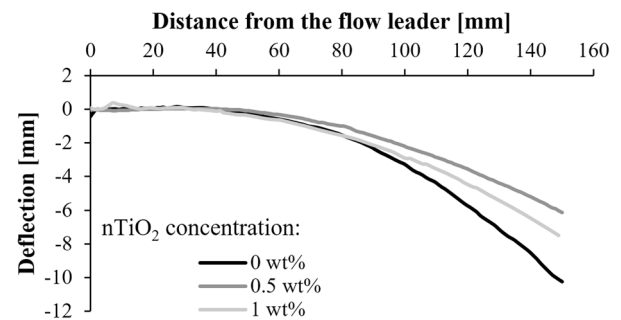


Fig. 16 The effect of the concentration of nano-sized TiO₂ on the warpage of the specimens

4 Conclusion

We have developed a novel eight-step In-Mold Coating procedure for Thermoplastic Resin Transfer Molding, which can be used to create a polyamide 6 matrix composite and its polyamide 6–based multifunctional surface coating in one production run. We have shown that the most critical step is to prepare the gap for the surface layer. If the base layer is in contact with ambient air (previously manufactured base or fully opened mold), moisture from the environment will block the polymerization near the contact surface, between the base layer and the coating. In this case, the two layers are separated after production. The remaining unpolymerized ϵ -caprolactam was detected by ATR-FTIR. SEM images confirmed that the reactive thermoplastic system had properly impregnated the reinforcements. Furthermore, we showed that no well-defined interface was formed between the base layer and the coating. Hence the polymer chains of the surface layer were bonded properly to the base layer.

With the process we developed, samples were prepared with different production parameters. We examined the surface layer adhesion and the product's warpage. During the pull-off tests, we found that a thicker coating and reinforcement increased adhesion strength. This is because a more uniform stress distribution may have developed in the thicker and stiffer specimen. Adhesion also improved when the reaction time of the base layer was increased. It is because with a shorter reaction time, conversion was not complete in the base layer and the colder coating material stopped its polymerization. Thus, the polymer chains were shorter and it resulted in impaired adhesion. The filler in the coating reduced the pull-off strength by reducing the effective adhesive surface. To analyze the warping of the products, we developed a new evaluation method based on 3D scanning. Using this, we showed that the warping of the base layer can be significantly reduced with a thicker coating, a filler, or fabric reinforcement. We demonstrated that the warpage of the product can be significantly reduced by optimizing the production parameters.

The great advantage of this novel process is that volatile organic compound (VOC) emissions are significantly

reduced compared to conventional coating methods, due to the closed system. In addition, production cycle time is shortened, as the base layer and the coating are produced in one cycle, which means considerable savings in cost and energy. Thanks to the high automation of the process and the lightweight, multifunctional coated composite, this can be a very attractive technology for the automotive industry. Furthermore, since both the base layer and the coating are made from the same base material (thermoplastic polyamide 6), the complex composite product is recyclable, which can significantly reduce its environmental impact.

Funding

This work was supported by the National Research, Development and Innovation Office, Hungary (2018-1.3.1-VKE-2018-00001, OTKA FK138501). The research reported in this paper is part of project no. BME-NVA-02, implemented with the support provided by the Ministry of Innovation and Technology of Hungary from the National Research, Development and Innovation Fund, financed under the TKP2021 funding scheme. Project no. RRF-2.3.1-21-2022-00009, titled National Laboratory for Renewable Energy has been implemented with the support provided by the Recovery and Resilience Facility of the European Union within the framework of Programme Széchenyi Plan Plus. Prepared with the professional support of the Doctoral Student Scholarship Program of the co-operative doctoral program of the Ministry for Innovation and Technology from the source of the National Research, Development and Innovation Fund. Project no. TKP2021-NKTA-07 has been implemented with the support provided by the Ministry of Culture and Innovation from the National Research, Development and Innovation Fund, financed under the TKP2021 funding scheme.

Acknowledgements

The authors would like to express their thanks Péter Pómlényi (HD Composite Zrt.) for his continuous support in measurements and evaluations. The authors thank HD Composite Zrt. for using the T-RTM equipment.

References

- [1] Matthews, C., Moran, F., Jaiswal, A. K. "A review on European Union's strategy for plastics in a circular economy and its impact on food safety", *Journal of Cleaner Production*, 283, 125263, 2021. <https://doi.org/10.1016/j.jclepro.2020.125263>
- [2] Cardamone, G. F., Ardolino, F., Arena, U. "Can plastics from end-of-life vehicles be managed in a sustainable way?", *Sustainable Production and Consumption*, 29, pp. 115–127, 2022. <https://doi.org/10.1016/j.spc.2021.09.025>

- [3] Kuwashiro, S., Nakao, N., Matsuda, S., Kakibe, T., Kishi, H. "Ionic cross-linked methacrylic copolymers for carbon fiber reinforced thermoplastic composites", *Express Polymer Letters*, 16(2), pp. 116–129, 2022.
<https://doi.org/10.3144/expresspolymlett.2022.10>
- [4] Zhang, X. Q., Hu, G. L., Cen, L., Lei, C. H. "Enhancing interfacial properties of carbon fiber/polyamide 6 composites by *in-situ* growing polyphosphazene nanotubes", *Express Polymer Letters*, 15(9), pp. 878–886, 2021.
<https://doi.org/10.3144/expresspolymlett.2021.70>
- [5] Bhudolia, S. K., Gohel, G., Subramanyam, E. S. B., Leong, K. F., Gerard, P. "Enhanced impact energy absorption and failure characteristics of novel fully thermoplastic and hybrid composite bicycle helmet shells", *Materials & Design*, 209, 110003, 2021.
<https://doi.org/10.1016/j.matdes.2021.110003>
- [6] Lendvai, L. "Water-Assisted Production of Polypropylene/Boehmite Composites", *Periodica Polytechnica Mechanical Engineering*, 64(2), pp. 128–135, 2020.
<https://doi.org/10.3311/PPme.13981>
- [7] Barnett, P. R., Cook, Z. A., Hulett, B. M., Varma, N. H., Penumadu, D. "Influence of processing parameters on permeability and infiltration of compression molded discontinuous carbon fiber organosheet composites", *Composites Part A: Applied Science and Manufacturing*, 152, 106682, 2022.
<https://doi.org/10.1016/j.compositesa.2021.106682>
- [8] Danezis, A., Williams, D., Edwards, M., Skordos, A. A. "Heat transfer modelling of flashlamp heating for automated tape placement of thermoplastic composites", *Composites Part A: Applied Science and Manufacturing*, 145, 106381, 2021.
<https://doi.org/10.1016/j.compositesa.2021.106381>
- [9] Murray, J. J., Robert, C., Gleich, K., McCarthy, E. D., Ó Brádaigh, C. M. "Manufacturing of unidirectional stitched glass fabric reinforced polyamide 6 by thermoplastic resin transfer moulding", *Materials & Design*, 189, 108512, 2020.
<https://doi.org/10.1016/j.matdes.2020.108512>
- [10] Bhudolia, S. K., Gohel, G., Kantipudi, J., Leong, K. F., Gerard, P. "Manufacturing and investigating the load, energy and failure attributes of thin ply carbon/Elium® thermoplastic hollow composites under low-velocity impact", *Materials & Design*, 206, 109814, 2021.
<https://doi.org/10.1016/j.matdes.2021.109814>
- [11] Obande, W., Mamalis, D., Ray, D., Yang, L., Ó Brádaigh, C. M. "Mechanical and thermomechanical characterisation of vacuum-infused thermoplastic- and thermoset-based composites", *Materials & Design*, 175, 107828, 2019.
<https://doi.org/10.1016/j.matdes.2019.107828>
- [12] Ageyeva, T., Sibikin, I., Karger-Kocsis, J. "Polymers and related composites via anionic ring-opening polymerization of lactams: Recent developments and future trends", *Polymers*, 10(4), 357, 2018.
<https://doi.org/10.3390/polym10040357>
- [13] Maazouz, A., Lamnawar, K., Dkier, M. "Chemorheological study and in-situ monitoring of PA6 anionic-ring polymerization for RTM processing control", *Composites Part A: Applied Science and Manufacturing*, 107, pp. 235–247, 2018.
<https://doi.org/10.1016/j.compositesa.2018.01.007>
- [14] Osváth, Z., Szőke, A., Pásztor, S., Závoczi, L., Szarka, G., Iván, B. "Recent Advances in the Synthesis and Analysis of Polyamide 6 and Products therefrom: From Polymerization Chemistry of ϵ -Caprolactam to Thermoplastic Resin Transfer Moulding (T-RTM)", *Academic Journal of Polymer Science*, 4(1), pp. 00118–00122, 2020.
<https://doi.org/10.19080/AJOP.2020.04.555629>
- [15] Semperger, O. V., Suplicz, A. "The Effect of the Parameters of T-RTM on the Properties of Polyamide 6 Prepared by in Situ Polymerization", *Materials*, 13(1), 4, 2020.
<https://doi.org/10.3390/ma13010004>
- [16] Vicard, C., De Almeida, O., Cantarel, A., Bernhart, G. "Experimental study of polymerization and crystallization kinetics of polyamide 6 obtained by anionic ring opening polymerization of ϵ -caprolactam", *Polymer*, 132, pp. 88–97, 2017.
<https://doi.org/10.1016/j.polymer.2017.10.039>
- [17] van Rijswijk, K., Bersee, H. E. N., Jager, W. F., Picken, S. J. "Optimisation of anionic polyamide-6 for vacuum infusion of thermoplastic composites: choice of activator and initiator", *Composites Part A: Applied Science and Manufacturing*, 37(6), pp. 949–956, 2006.
<https://doi.org/10.1016/j.compositesa.2005.01.023>
- [18] Yan, C., Li, H., Zhang, X., Zhu, Y., Fan, X., Yu, L. "Preparation and properties of continuous glass fiber reinforced anionic polyamide-6 thermoplastic composites", *Materials & Design*, 46, pp. 688–695, 2013.
<https://doi.org/10.1016/j.matdes.2012.11.034>
- [19] Wilhelm, M., Wendel, R., Aust, M., Rosenberg, P., Henning, F. "Compensation of water influence on anionic polymerization of ϵ -caprolactam: 1. Chemistry and Experiments", *Journal of Composites Science*, 4(1), 7, 2020.
<https://doi.org/10.3390/jcs4010007>
- [20] Miranda Campos, B., Bourbigot, S., Fontaine, G., Bonnet, F. "Thermoplastic matrix-based composites produced by resin transfer molding: A review", *Polymer Composites*, 43(5), pp. 2485–2506, 2022.
<https://doi.org/10.1002/pc.26575>
- [21] Gomez, C., Salvatori, D., Caglar, B., Trigueira, R., Orange, G., Michaud, V. "Resin Transfer molding of High-Fluidity Polyamide-6 with modified Glass-Fabric preforms", *Composites Part A: Applied Science and Manufacturing*, 147, 106448, 2021.
<https://doi.org/10.1016/j.compositesa.2021.106448>
- [22] Murray, J. J., Bajpai, A., Quinn, J., McClements, J., Gleich, K., McCarthy, E. D., Ó Brádaigh, C. M. "Effect of glass fibre sizing on the interfacial properties of composites produced using in-situ polymerised Polyamide-6 transfer moulding", *Composites Part B: Engineering*, 235, 109743, 2022.
<https://doi.org/10.1016/j.compositesb.2022.109743>
- [23] Irisawa, T., Shibata, M., Yamamoto, T., Tanabe, Y. "Effects of carbon nanofibers on carbon fiber reinforced thermoplastics made with in situ polymerizable polyamide 6", *Composites Part A: Applied Science and Manufacturing*, 138, 106051, 2020.
<https://doi.org/10.1016/j.compositesa.2020.106051>

- [24] Höhne, C.-C., Wendel, R., Käbisch, B., Anders, T., Henning, F., Kroke, E. "Hexaphenoxycyclotriphosphazene as FR for CFR anionic PA6 via T-RTM: a study of mechanical and thermal properties", *Fire and Materials*, 41(4), pp. 291–306, 2017.
<https://doi.org/10.1002/fam.2375>
- [25] de With, G. (ed.) "Application Methods", In: *Polymer Coatings: Guide to Chemistry, Characterization, and Selected Applications*, Wiley-VCH, 2018. pp. 135–153. ISBN 9783527806324
<https://doi.org/10.1002/9783527806324.ch6>
- [26] Rogers, W., Hoppins, C., Gombos, Z., Summerscales, J. "In-mould gel-coating of polymer composites: a review", *Journal of Cleaner Production*, 70, pp. 282–291, 2014.
<https://doi.org/10.1016/j.jclepro.2014.01.091>
- [27] Dinh, T.-V., Son, Y.-S., Choi, I.-Y., Song, K.-Y., Sunwoo, Y., Kim, J.-C. "Emissions of volatile organic compounds associated with painting methods and an estimation of the α -dicarbonyl formation potential", *International Journal of Environmental Science and Technology*, 16(8), pp. 3961–3970, 2019.
<https://doi.org/10.1007/s13762-018-2100-5>
- [28] Chen, X., Bhagavatula, N., Castro, J. M. "In-mold coating (IMC) process for thermoplastic parts", *AIP Conference Proceedings*, 712, pp. 174–179, 2004.
<https://doi.org/10.1063/1.1766519>
- [29] Kovács, Z., Pomázi, Á., Toldy, A. "The flame retardancy of polyamide 6-prepared by in situ polymerisation of ϵ -caprolactam – For T-RTM applications", *Polymer Degradation and Stability*, 195, 109797, 2022.
<https://doi.org/10.1016/j.polymdegradstab.2021.109797>
- [30] Mallick, P. K. "Composites Engineering Handbook", CRC Press, 1997. ISBN 9780429175497
<https://doi.org/10.1201/9781482277739>
- [31] Bhuyan, M. S. K., Ko, S., Villarreal, M. G., Straus, E. J., James, L., Castro, J. M. "Decreasing the cycle time for in-mold coating (IMC) of sheet molding compound (SMC) compression molding", *Polymer Engineering and Science*, 59(6), pp. 1158–1166, 2019.
<https://doi.org/10.1002/pen.25095>
- [32] Rayle, J. W., Cassil, D. W. "Advancements in injection in-mold coating technology", *Metal Finishing*, 93(9), pp. 41–44, 1995.
[https://doi.org/10.1016/0026-0576\(95\)99499-Z](https://doi.org/10.1016/0026-0576(95)99499-Z)
- [33] Gombos, Z. J., Summerscales, J. "In-mould gel-coating for polymer composites", *Composites Part A: Applied Science and Manufacturing*, 91(1), pp. 203–210, 2016.
<https://doi.org/10.1016/j.compositesa.2016.10.014>
- [34] Boros, R., Sibikin, I., Ageyeva, T., Kovács, J. G. "Development and Validation of a Test Mold for Thermoplastic Resin Transfer Molding of Reactive PA-6", *Polymers*, 12(4), 976, 2020.
<https://doi.org/10.3390/polym12040976>
- [35] Semperger, O. V., Osváth, Z., Pásztor, S., Suplicz, A. "The effect of the titanium dioxide nanoparticles on the morphology and degradation of polyamide 6 prepared by anionic ring-opening polymerization", *Polymer Engineering and Science*, 62(6), pp. 2079–2088, 2022.
<https://doi.org/10.1002/pen.25990>
- [36] Mondragon, G., Kortaberria, G., Mendiburu, E., González, N., Arbelaiz, A., Peña-Rodríguez, C. "Thermomechanical recycling of polyamide 6 from fishing nets waste", *Journal of Applied Polymer Science*, 137(10), 48442, 2020.
<https://doi.org/10.1002/app.48442>
- [37] Farias-Aguilar, J. C., Ramírez-Moreno, M. J., Téllez-Jurado, L., Balmori-Ramírez, H. "Low pressure and low temperature synthesis of polyamide-6 (PA6) using Na⁰ as catalyst", *Materials Letters*, 136, pp. 388–392, 2014.
<https://doi.org/10.1016/j.matlet.2014.08.071>
- [38] Wendel, R., Rosenberg, P., Wilhelm, M., Henning, F. "Anionic Polymerization of ϵ -Caprolactam under the Influence of Water: 2. Kinetic Model", *Journal of Composite Science*, 4(1), 8, 2020.
<https://doi.org/10.3390/jcs4010008>
- [39] Semperger, O. V., Suplicz, A. "The effect of titanium dioxide on the moisture absorption of polyamide 6 prepared by T-RTM", *IOP Conference Series: Materials Science and Engineering*, 903, 012009, 2020.
<https://doi.org/10.1088/1757-899X/903/1/012009>
- [40] Osváth, Z., Szöke, A., Pásztor, S., Szarka, G., Závoczki, L. B., Iván, B. "Post-Polymerization Heat Effect in the Production of Polyamide 6 by Bulk Quasiliving Anionic Ring-Opening Polymerization of ϵ -Caprolactam with Industrial Components: A Green Processing Technique", *Processes*, 8(7), 856, 2020.
<https://doi.org/10.3390/pr8070856>
- [41] Awang, M., Wan Mohd, W. R. "Comparative studies of Titanium Dioxide and Zinc Oxide as a potential filler in Polypropylene reinforced rice husk composite", *IOP Conference Series: Materials Science and Engineering*, 342, 012046, 2018.
<https://doi.org/10.1088/1757-899X/342/1/012046>